ONIX Results: Comparison of Grid Geometry (BATMAN - ELISE - Flat Grid)

Adrien Revel[1,a)], Serhiy Mochalskyy[1], Dirk Wünderlich[1], Ursel Fantz[1] and Tiberiu Minea[2]

[1]*Max-Planck Institut für Plasmaphysik, Garching, Germany.*
[2]*LPGP, CNRS, Univ. Paris-Sud, Université Paris-Saclay, Orsay, France.*

[a)]Corresponding author: adrien.revel@u-psud.fr

Abstract. The 3D PIC-MCC code ONIX is dedicated to the modelling of negative hydrogen or deuterium ion extraction and the co-extracted electrons from the plasma in radio-frequency driven sources. The extraction process highly depends on the plasma characteristics close to the plasma grid where it is difficult to obtain experimental data. ONIX brings valuable insights on the plasma behavior in this area. In the code, the numerical treatment of the boundaries have been improved in order to describe with more accuracy the potential and the electric field in this vicinity. The computation time has been reduced by a factor of 2 and the parallelization efficiency has been highly improved. The influence of the magnetic field in BATMAN on the plasma behaviour has been investigated by comparing two different configurations of the magnet bars producing the filter field (internal magnets: $x = 3$ cm; external magnets: $x = 9$ cm). A flat grid geometry for the PG instead of the usual conical grid geometry has been studied to evaluate its impact on the extracted current, especially for the negative ions emitted from the surface of the PG. Finally, the ONIX code has been used for the first 3D PIC calculations ever performed for the ELISE experiment.

INTRODUCTION

The future international thermonuclear experimental reactor (ITER) will require additional heating devices to reach a self-sustained nuclear fusion reaction and for the current drive. Two Neutral Beam Injectors (NBI) should deliver a total power of 33 MW by injecting a neutral beam of hydrogen or deuterium at 870 keV or 1 MeV, respectively, during a pulse length of 1 hour [1, 2]. The ITER NBI will be based on negative ions due to their higher neutralization efficiency at 1 MeV.

Two experimental radio-frequency (RF) negative ion source prototypes for the ITER NBIs are being operated at Max-Planck Institute für Plasmaphysik in Garching, Germany. The prototype source (in the BATMAN test facility) is equipped with one driver which is 1/8 of the size of the source in ITER and is a positive ion based source. ELISE is equipped with 4 drivers corresponding to half the size of the ITER sources [3, 4] and is specifically designed for the production and extraction of negative ions. The full size ITER NBI experiments, namely SPIDER (Source for Production of Ion of Deuterium Extracted from RF plasma) and MITICA (Megavolt ITER Injector & Concept Advancement), are under construction at the Neutral Beam Test Facility (NBTF) in Padova, Italy, and are expected to deliver the requirements needed for ITER operations (extracted negative ion current of: $J_{H^-} = 329$ Am^{-2}, $J_{D^-} = 286$ Am^{-2}).

The negative ion sources consist of four main parts: the driver, the expansion chamber, the extraction system and a first stage acceleration grid. The driver generates a plasma ($n_e \approx 10^{18}$ m^{-3}, $T_e \approx 10$ eV) by inductively coupled radio-frequency coils which diffuses into the expansion chamber. A magnetic field, generated either by permanent magnets or by a current flowing through the plasma grid, decreases the electron temperature to 1 eV. Negative ions are produced mainly by surface conversion of atoms impinging on a caesium covered surface (surface production). Then, they are extracted and accelerated by an electric field as well as co-extracted electrons.

The extraction process involves complex physics. The trajectories of the particles in the plasma are subject to intricate induced 3D electromagnetic fields, kinetic reactions and plasma-surface processes. Negative ions must be extracted properly (*i.e.* with a low emittance) in order to optimize the further beam transport. The shape and the

position of the meniscus (plasma-beam frontier) are key parameters for the beam formation and its optics. Moreover, due to the high emission rate of negative ions from the caesium covered surface of the plasma grid, a negative potential well (virtual cathode) forms close to the surface pushing them back towards the plasma grid [5]. Depending on where the negative ions are emitted, they can either be subject to the potential well or they can be directly extracted (see Fig. 1). The extraction process constitutes one of the most crucial steps for NBI transmittance and efficiency. The lack of experimental data near the plasma grid (< 1 cm) makes it difficult to fully understand the physics involved.

During the last several years, the 3D PIC-MCC ONIX (Orsay Negative Ion eXtraction) code has been dedicated to the modelling of the extraction of negative hydrogen ions and co-extracted electrons. The code is benchmarked with direct comparison to experimental results obtained at BATMAN and provides valuable insight on the extraction process close to the plasma grid [6]. In this paper, the first part will describe the ONIX code and its numerical features, the second part will show results of different magnetic field conditions and different geometries in the BATMAN test facility. The first results on ELISE using the ONIX code are shown in the third section and finally, the last section will summarize the results and describe future works.

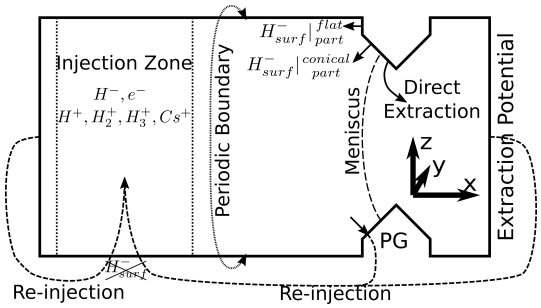

FIGURE 1. Schematic view of the simulation domain used in ONIX with a double chamfered extraction aperture. The simulation starts with an initial bulk plasma in the injection zone. Negative ions are emitted from the PG surface. Periodic boundary conditions in y and z are applied. A particle coming from the bulk plasma hitting either the left or the right boundary is re-injected **contrarily to the negative ions coming from the surface.**

Numerical approach

ONIX is a 3D PIC-MCC code created for studying the extraction process in negative ion sources. [7, 8, 9]. Due to computation time constraint, the simulation domain is limited to one aperture around the Plasma Grid (PG) by applying periodic boundary conditions in the transverse direction of the beam, namely, y and z. The simulation domain includes a bulk plasma, a plasma grid and an extraction potential at the right side of the domain as shown in Fig. 1.

The code starts with an initial density of H^-, e^-, H^+, H_2^+, H_3^+, Cs^+ in the bulk plasma which evolves over time. Particles hitting the right or left boundary or the PG are re-injected into that injection zone.

H^- are injected in the simulation domain from the inner surfaces (flat and conical part) of the PG to reproduce the surface conversion process at the caesium covered surface [10, 11]. All particles are injected according to a Maxwellian distribution function for a given temperature. Note that the negative ions coming from the bulk plasma are called H^-_{bulk} to distinguish them from those emitted from the flat H^-_{flat} or conical H^-_{conus} surface.

In order to decrease the co-extracted electron current, a magnetic filter field is present in the source. In the 1/8 prototype source, the filter field is created either by internal permanent magnets placed at a distance from the PG of 3 cm hereafter referred to as the 'x = 3 cm' case or by an external movable (along the beam direction) magnet frame placed at a distance from the PG between 9 and 19 cm. The position of 9 cm is hereafter referred to as the '9 cm' case. The filter field dominates in the source and the bulk plasma. Its main purpose is to reduce the electron temperature in the expansion chamber but it also decreases the amount of co-extracted electrons. An additional deflecting field perpendicular to the filter field is created by permanent magnets embedded in the extraction grid and used to remove the co-extracted electrons from the beam before they reach a too high energy and risk damaging beamline components.

The PIC algorithm is subject to several stability criteria. Among them, to ensure no numerical heating, the mesh size must be smaller than the Debye length [12]. This criterion is very difficult to fulfill for 3D simulations of dense plasma evolving in a large domain. The mesh size used in ONIX is between 4 to 5 times larger than the Debye length.

It is a compromise between the computation time and this criterion. Although the accuracy of the results could be questioned, the results still provide beneficial insights to the physics in play.

To reduce the computation time, the code has been parallelized using the MPI library via a spatial decomposition domain. Recent improvements have reduced the computation time by a factor of 2 and drastically improved the scalability of the code when using more threads (tested up to 128 threads). Furthermore, ONIX has been improved to make it more flexible to use. The complex geometry interpolation of the plasma grid has been automated so it is now easier to change its shape. Furthermore, the geometry of the plasma grid used at ELISE has been added to the code.

Finally, the accuracy of the potential and electric field around the boundaries (right/left plane or grid) has been improved by introducing a refined interpolation routine of the electric field close to the surfaces in order to better describe the particle motion in its vicinities. This point will be discussed in a future paper.

RESULTS IN BATMAN CONFIGURATION

BATMAN configuration

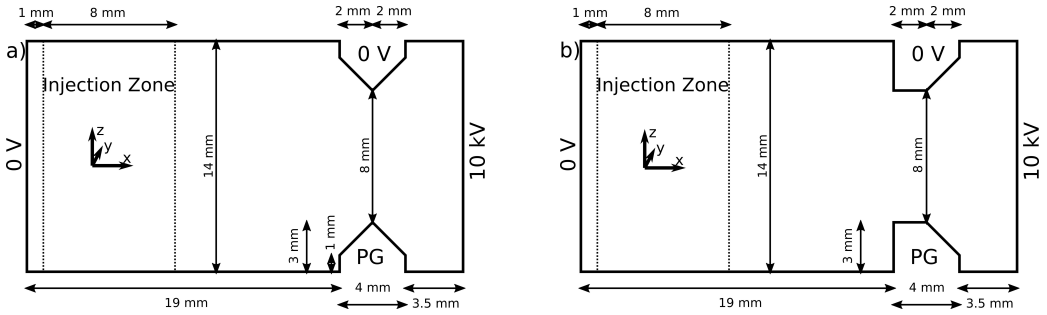

FIGURE 2. Dimension of the simulation domain used in ONIX for BATMAN with the conical grid shown on the left. The image on the right shows how a flat grid is taken into account.

The calculation domain used for simulating the vicinity of one extraction aperture in BATMAN is shown in Fig. 2.a [13]. The size of the simulation domain is $28 \times 14 \times 14$ mm. The distance between the left boundary and the plasma grid is 19.1 mm. The aperture radius is 4 mm which gives a 50 mm^2 aperture surface. The mesh size is $75 \times 100 \times 100$ µm. The extraction potential plane is placed at a distance of 3.5 mm from the PG. The extracted currents are calculated at this plane.

The initial density of each species is: $n_{e^-} = 1.33 \times 10^{17}$ m^{-3}, $n_{H^-} = n_e/2$, $n_{H^+} = 0.833 \times 10^{17}$ m^{-3}, $n_{H_2^+} = 0.833 \times 10^{17}$ m^{-3}, $n_{H_3^+} = 0.25 \times 10^{17}$ m^{-3} and $n_{Cs^+} = 0.0833 \times 10^{17}$ m^{-3}. Theses values correspond to a particular experimental condition [14, 15], where the plasma is dominated by negative ions, different from previous calculations [8]. In this contribution, ion-ion plasma refers to the situation where more than half of the negatively charged particles are negative ions. The higher the amount of NI, the stronger the ion-ion plasma is. The negative ion emission rate from the inner conical and flat surface is 550 Am^{-2}. The extraction potential is set at 10 kV (although the grid of BATMAN has the optimum perveance at 5 kV for ITER relevant current density of extracted negative ions) and the PG is biased at 0 V.

Influence of the magnetic filter field

As mentioned before, the magnetic filter field is created either by internal ($x = 3$ cm) or external ($9 < x < 19$ cm) permanent magnets placed outside the chamber between the driver and the PG. Figure 3 shows the complex structure of the magnetic field in the simulation domain for a) $B_y : x = 3$ cm, b) $B_y : x = 9$ cm, c) $B_z : x = 3$ cm and d) $B_z : x = 9$ cm.

The main component of the filter field is along the y direction while the main component of the deflecting field is along the z direction. Thus, the z component of the magnetic field close to the PG is almost identical for both cases (Fig. 3.c and 3.d). However, the filter field is affected by the position of the magnets (Fig. 3.a and 3.b). Obviously, the

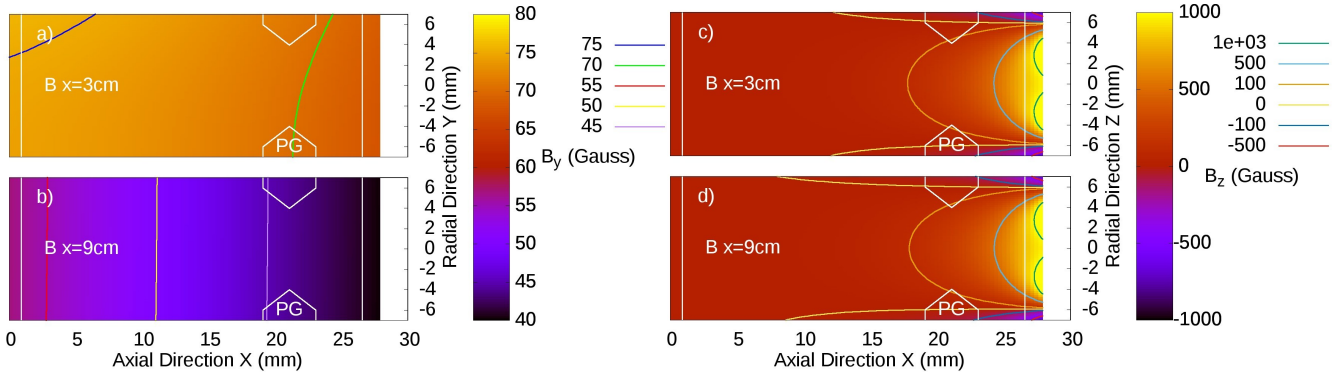

FIGURE 3. Magnetic field used in BATMAN simulation for two positions of the permanent magnet, a & c: $x = 3$ cm, b & d: $x = 9$ cm ; for two components, a & b: y component, c & d: z component. Note that the color scales are different in each image.

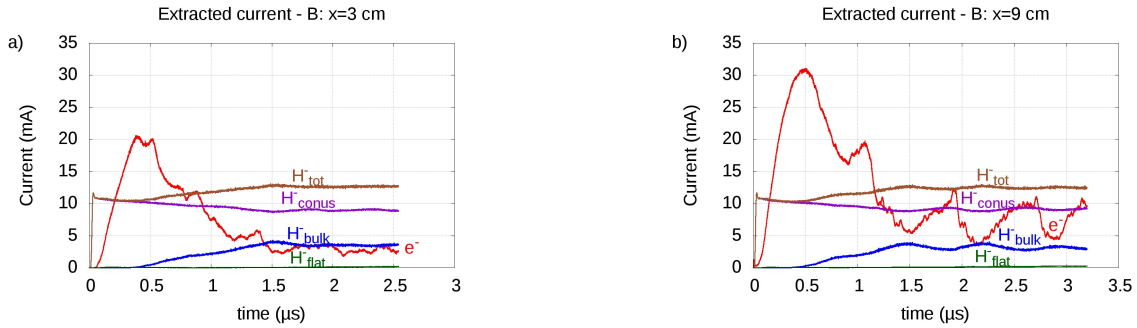

FIGURE 4. Extracted current of electrons (e^-), of the negative ions coming from the bulk plasma (H^-_{bulk}), from the flat surface of the PG (H^-_{flat}), from the conical surface of the PG (H^-_{conus}) and of all negative ions (H^-_{tot}) for two different magnetic field configurations, a: $x = 3$ cm and b: $x = 9$ cm.

filter filed strength close to the PG is lower when the magnets are placed further away. In the vicinity of the grid, 3D topology of the deflection field dominates.

Figure 4 shows the extracted current as a function of computational time for $x = 3$ cm and $x = 9$ cm. The extracted current of negative ions is identical for both cases. However, the co-extracted electron current is oscillating between 5 and 10 mA in the $x = 9$ cm case while it is constant at 3 mA in the $x = 3$ cm case. Despite the oscillations in the $x = 3$ cm case, a higher electron current is obtained than for the $x = 3$ cm case. Both observations, i.e. similar ion current but higher electron current, are in agreement with what has been obtained experimentally [16].

Figure 5 shows the profile of the density of the positive ions, negative ions and electrons along the beam direction in the middle of the aperture ($z = 0$ mm, $y = 0$ mm) for both cases at $t = 2.5$ µs. In accordance with the lower co-extracted electron current, there are less electrons close to the PG for the case $x = 3$ cm. Moreover, the ion-ion plasma region is more pronounced in this case. This change of the magnetic field close to the extraction aperture does not affect the extracted current or the beam profile as the meniscus remains the same, confirming again that the deflection field is dominant at this position.

Influence of the grid geometry flat vs conical

The flat grid geometry is shown in Fig. 2.b. The inner conical part has been replaced by a cylinder in order to keep the dimension as close as possible to the conical geometry. The initial density, the biased potential and the extraction potential are kept the same. The negative ion emission rate is 550 Am^{-2} as before but negative ions are only emitted from the inner flat part. The magnetic field used in this case is the one corresponding to the $x = 3$ cm case. Here, the mesh size is $70 \times 70 \times 70$ µm.

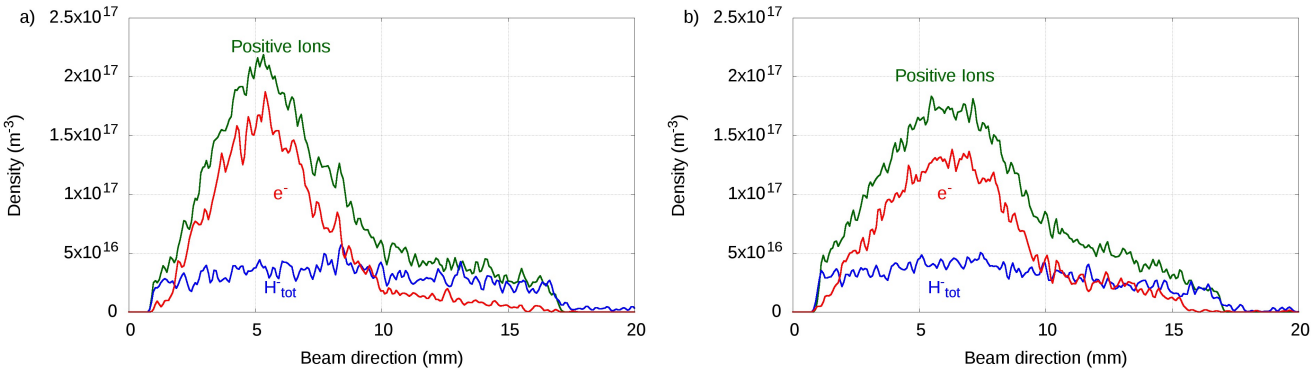

FIGURE 5. Profile of the density of the positive species, negative ions and electrons along the beam direction in the middle of the aperture (y = 0 mm, z = 0 mm) for two different magnetic field configurations, a: x = 3 cm and b: x = 9 cm.

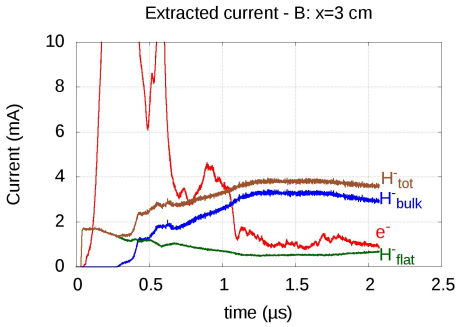

FIGURE 6. Flat grid: extracted current of electrons (e^-), of the negative ions coming from the bulk plasma (H^-_{bulk}), from the flat surface of the PG (H^-_{flat}) and of all negative ions (H^-_{tot}).

Figure 6 shows the evolution of the extracted current over time. The total negative ion extracted current is 3-4 times smaller in this case even though the total number of negative ions emitted from the surface is roughly the same (when compared to the amount emitted in the conical grid). Because of the position and the shape of the meniscus (Fig. 7 – red line), a lower amount of negative ions is directly extracted. However, the extraction from the flat part has only been increased by a factor of 4 (0.16 mA in conical geometry, 0.7 mA in flat geometry) although the flat surface has only been increased by a factor of 2. The co-extracted electron current is $\sim$ 1 mA, 3 times smaller than for the conical grid. An ion-ion plasma is forming close to the meniscus, similar to the one observed for the x = 3 cm conical grid case in BATMAN.

Figure 7 shows the H^- density of the negative ions produced from a) the flat surface b) the bulk plasma. The negative ions coming from the bulk plasma produce a perfectly collimated beam while the negative ions coming from the flat surface produce a ring-shaped beam due to their over-convergence.

RESULTS IN ELISE CONFIGURATION

ELISE configuration

Figure 8 shows the geometry of the calculation domain in the middle plane used for simulating the H^- extraction and the e^- co-extraction at ELISE [17]. The flat surface is in this case very small, S_{flat} = 11.3 mm^2 in comparison to the conical surface, S_{conus} = 363 mm^2. Due to the larger size of the aperture and the compact arrangement of the apertures in the beamlet group, the width of the simulation domain is increased corresponding to a distance between two consecutive apertures of 20 mm. The extraction potential is 10 kV which corresponds to the optimum perveance

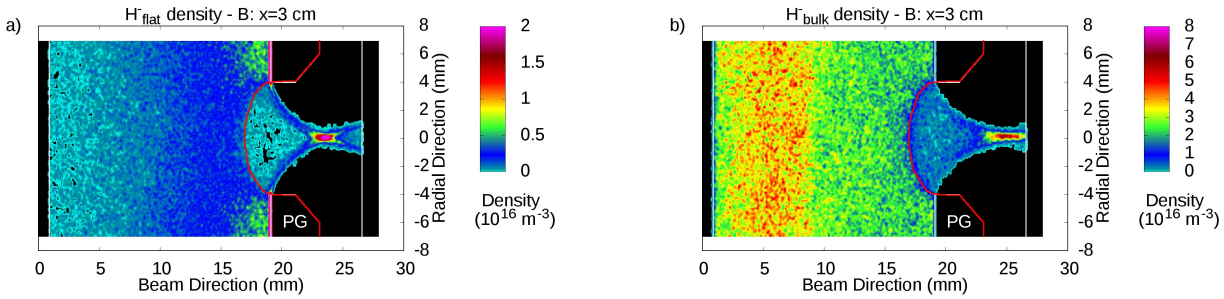

FIGURE 7. Density of H^- in the middle (x, y) plane ($z = 0$ mm). a: H^- coming from the flat surface and b: H^- coming from the bulk plasma. The red line indicates the position of the meniscus.

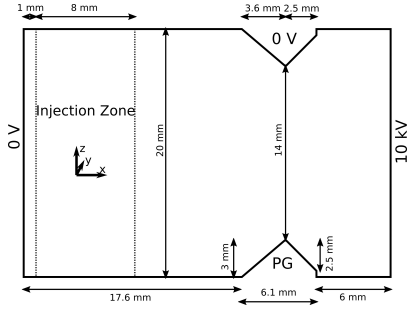

FIGURE 8. Dimension of the simulation domain used in ONIX for ELISE.

for an ITER relevant extracted current of negative ions .The initial density of the different species is the same as for the BATMAN simulation. The mesh size is $75\times125\times125$ µm. The treatment of the particles with the different boundaries is unchanged.

The magnetic field of ELISE is different from the one used in BATMAN. The deflecting field is still created by permanent magnets embedded in the EG but the filter field is created by a current flowing inside the PG ($I_{PG} < 5$ kA). Its strength can be controled with the applied current. Fig. 9 shows the magnetic field in the simulation domain for a current of $I_{PG} = 1$ kA for a: y component of the filter field, b: y component of the deflecting field, c: z component of the filter field, d: z component of the deflecting field. The y, resp. z, component of the deflecting field, resp. filter field, is almost zero as it can be expected due to the geometry of the grids and the magnets. The main difference with the magnetic field in the case for BATMAN (Fig. 3) comes from the filter field which is more curved and closer to the aperture since it is created by a current flowing in the PG. But also here, close to the grid, the deflection field is dominant.

Results

Figure 10 shows the extracted current of the different species over the computational time. The co-extracted current of electrons is about 1.6 mA which is lower than in the BATMAN case. The total extracted current of negative ions is 23.5 mA, about two times higher than in the BATMAN case. The current of negative ions coming from the flat surface is even lower than in BATMAN case due to the flat surface ($S_{flat} = 11.3$ mm^2). However, the current density of negative ions is 150 Am^{-2}, compared to 250 Am^{-2} in the BATMAN case. This preliminary result is in contradiction with experimental observations [18] where the current density is only dependant on the RF power. However, it has to be mentioned, that the code uses the same input parameter as for BATMAN. Thus, a systematic parameter study is the next step.

The density of negative ions generated at the conical part of the grid and from the bulk plasma is shown in Fig. 11. The surface of the conical grid affected by the direct extraction process (no potential well) is mostly the same

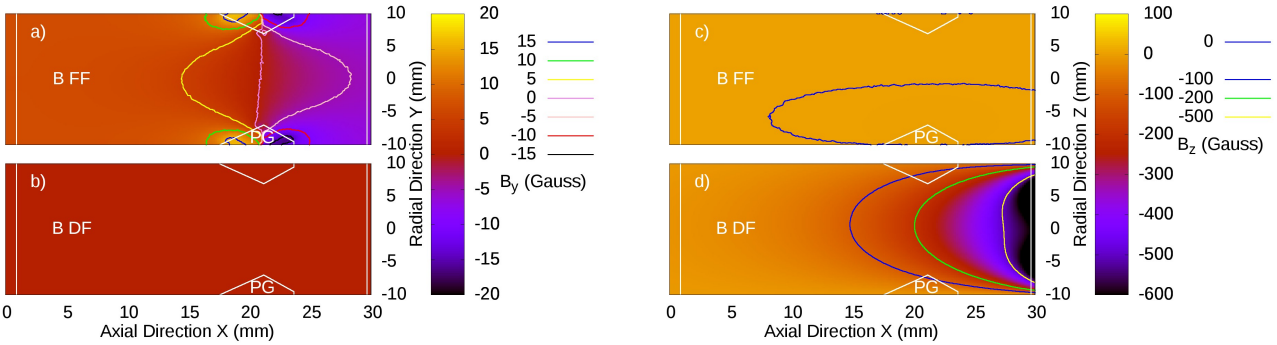

FIGURE 9. Magnetic field used in the ELISE simulation with a: y component of the filter field (B FF), b: y component of the deflecting field (B DF), c: z component of the filter field and d: d component of the deflecting field.

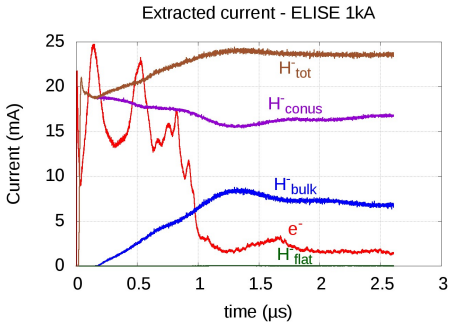

FIGURE 10. Extracted current of electrons (e^-), of the negative ions coming from the bulk plasma (H^-_{bulk}), from the flat surface of the PG (H^-_{flat}), from the conical surface of the PG (H^-_{conus}) and of all negative ions (H^-_{tot}) for the ELISE simulation.

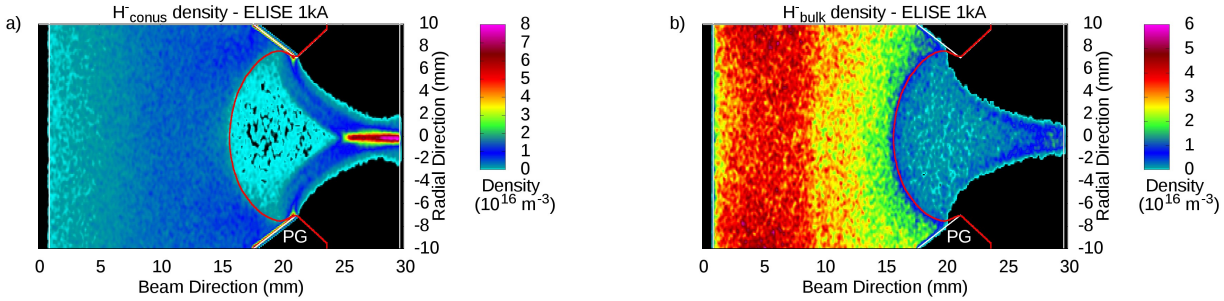

FIGURE 11. Density of H^- in the middle (x, y) plane (z = 0 mm) in the ELISE simulation with a: H^- coming from the conical surface and b: H^- coming from the bulk plasma. The red line indicates the position of the meniscus.

as for BATMAN. Thus, the extracted negative ion current does not scale with the surface of the conical part of the grid. Compared to BATMAN, the layout of the aperture is different. In ELISE, the apertures are arranged according to a matrix, while in BATMAN, each row has an offset of half an aperture. Due to the shape and the diposition of the apertures, there is no clear limit between two consecutive ones. Further investigation will follow.

CONCLUSION

The 3D PIC-MCC code ONIX has been improved in terms of accuracy (better description of the potential and electric field near the boundaries, especially at the PG) and in terms of performance (2 times faster and improved parallelization efficiency up to 128 threads).

ONIX has been used to compare the influence of the magnetic field in BATMAN on the plasma behaviour. The two different magnetic fields correspond to two different positions of the permanent magnets. The co-extracted electron current is lower and oscillating in the $x = 9$ cm case and the ion-ion plasma forming near the PG is more pronounced for the 3 cm case. Furthermore, ONIX has been used for the study of a flat geometry showing that the extracted negative ion current is dominated by the negative ions coming from the bulk plasma while the current of negative ions emitted from the inner flat surface remains low. ELISE simulation have been performed using ONIX for the first time. Although the beam is pefectly collimated, the extracted negative ion current density is lower than expected. The current density is supposed to be close to the results on BATMAN. The current however is twice as large as that in ELISE. As the plasma parameters have been kept the same, systematic parameter studies will follow.

Future work will be focused on the study the Debye legnth criterion and how it affects the plasma behavior and the extracted currents [19].

REFERENCES

[1] R. S. Hemsworth, A. Tanga, and V. Antoni, Review of Scientific Instruments **79** (2008).

[2] R. Hemsworth, H. Decamps, J. Graceffa, B. Schunke, M. Tanaka, M. Dremel, A. Tanga, H. D. Esch, F. Geli, J. Milnes, T. Inoue, D. Marcuzzi, P. Sonato, and P. Zaccaria, Nuclear Fusion **49**, p. 045006 (2009).

[3] U. Fantz, P. Franzen, W. Kraus, H. D. Falter, M. Berger, S. Christ-Koch, M. Fröschle, R. Gutser, B. Heinemann, C. Martens, P. McNeely, R. Riedl, E. Speth, and D. Wünderlich, Review of Scientific Instruments **79** (2008).

[4] B. Heinemann, U. Fantz, P. Franzen, M. Fröschle, M. Kircher, W. Kraus, C. Martens, R. Nocentini, R. Riedl, B. Ruf, L. Schiesko, C. Wimmer, and D. Wünderlich, Fusion Engineering and Design **88**, 512 – 516 (2013), proceedings of the 27th Symposium On Fusion Technology (SOFT-27); Liège, Belgium, September 24-28, 2012.

[5] D. Wünderlich, R. Gutser, and U. Fantz, Plasma Sources Science and Technology **18**, p. 045031 (2009).

[6] S. Mochalskyy, U. Fantz, D. Wünderlich, and T. Minea, Nuclear Fusion **56**, p. 106025 (2016).

[7] S. Mochalskyy, A. Lifschitz, and T. Minea, Nuclear Fusion **50**, p. 105011 (2010).

[8] S. Mochalskyy, D. Wnderlich, B. Ruf, U. Fantz, P. Franzen, and T. Minea, Plasma Physics and Controlled Fusion **56**, p. 105001 (2014).

[9] S. Mochalskyy, D. Wünderlich, U. Fantz, P. Franzen, and T. Minea, Nuclear Fusion **55**, p. 033011 (2015).

[10] M. Bacal, Nuclear Fusion **46**, p. S250 (2006).

[11] Y. Belchenko, G. Dimov, and V. Dudnikov, Nuclear Fusion **14**, p. 113 (1974).

[12] C. K. Birdsall and A. B. Langdon, *Plasma physics via computer simulation*, Series in plasma physics (Taylor & Francis, New York, 2005) originally published: New York ; London : McGraw-Hill, 1985.

[13] E. Speth *et al.*, Nucl. Fusion **46**, S220–S238 (2006).

[14] P. McNeely and L. Schiesko, Review of Scientific Instruments **81** (2010).

[15] C. Wimmer, U. Fantz, and NNBI-Team, AIP Conference Proceedings **1515** (2013).

[16] P. Franzen, L. Schiesko, M. Frschle, D. Wünderlich, U. Fantz, and the NNBI Team, Plasma Physics and Controlled Fusion **53**, p. 115006 (2011).

[17] B. Heinemann *et al.*, Fusion Engineering and Design **84**, 915–922 (2009).

[18] U. Fantz, B. Heinemann, D. Wünderlich, R. Riedl, W. Kraus, R. Nocentini, and F. Bonomo, Review of Scientific Instruments **87** (2016), http://dx.doi.org/10.1063/1.4932560.

[19] J. P. Boeuf, G. Fubiani, and L. Garrigues, Plasma Sources Science and Technology **25**, p. 045010 (2016).